

Constrained Differential Dynamic Programming Revisited

Yuichiro Aoyama^{1,2}, George Boutselis¹, Akash Patel¹, and Evangelos A. Theodorou¹

¹School of Aerospace Engineering, Georgia Institute of Technology, Atlanta, GA, USA

²Komatsu Ltd., Tokyo, Japan

{yaoyama3, apatel435, gbouts, evangelos.theodorou}@gatech.edu

Abstract—Differential Dynamic Programming (DDP) has become a well established method for unconstrained trajectory optimization. Despite its several applications in robotics and controls however, a widely successful constrained version of the algorithm has yet to be developed. This paper builds upon penalty methods and active-set approaches, towards designing a Dynamic Programming-based methodology for constrained optimal control. Regarding the former, our derivation employs a constrained version of Bellman’s principle of optimality, by introducing a set of auxiliary slack variables in the backward pass. In parallel, we show how Augmented Lagrangian methods can be naturally incorporated within DDP, by utilizing a particular set of penalty-Lagrangian functions that preserve second-order differentiability. We demonstrate experimentally that our extensions (individually and combinations thereof) enhance significantly the convergence properties of the algorithm, and outperform previous approaches on a large number of simulated scenarios.

I. INTRODUCTION

Trajectory optimization problems arise very frequently in robotics and controls applications. Examples include finding suitable motions for robotic grasping and manipulation tasks [7], or minimizing fuel for orbital transfers [8]. Mathematically speaking, such problems require computing a state/control sequence that minimizes a specified cost function, while satisfying the dynamics constraints of the agent. Common methodologies for trajectory optimization rely on optimal control and/or optimization theory. The former approach provides fundamental principles for obtaining solutions (based, for example, on Dynamic Programming or the Hamilton-Jacobi-Bellman equation), which, however, do not scale well with high-dimensional, nonlinear problems [1]. In contrast, standard direct optimization methods can be used for discrete optimal control [14]. The main drawback of these works is that feasibility with respect to dynamics has to be explicitly imposed, thus slowing down the optimization process [21].

One of the most successful trajectory optimization algorithms is Differential Dynamic Programming (DDP), originally developed by Jacobson and Mayne [5]. DDP is an indirect method which utilizes Bellman’s principle of optimality to split the problem into “smaller” optimization subproblems at each time step. Under mild assumptions on the cost and dynamics, it can be shown that DDP achieves locally quadratic convergence rates [11]. While the original method relies on

second-order derivatives, one of its variations, iterative-Linear-Quadratic-Regulator (iLQR), uses only Gauss-Newton approximations of the cost Hessians as well as first-order expansions of the dynamics [10], which is often numerically advantageous. The aforementioned algorithms have been employed in various applications such as robotic manipulation [7], bipedal walking [15] and model-based reinforcement learning [9], to name a few.

While unconstrained DDP has been widely tested and used over the past decades, its constrained counterpart has yet to be properly established. Since most practical applications in controls and robotics include state and/or control constraints (e.g., navigating through obstacles, respecting joint/actuator limits, etc.), off-the-shelf optimization solvers still remain the most popular tool for trajectory optimization among scientists and practitioners [6, 14]. A few works have attempted to extend the DDP framework to the constrained case. [20, 16] considered the case of control bounds by solving several quadratic programs over the trajectory, and [3] dealt with equality constraints only via projection techniques. The works in [8, 21] utilized the Karush-Kuhn-Tucker (KKT) conditions when both state and control constraints are present, with [21], [12], in particular, solving successive quadratic programs in the forward pass of the method. [8, 18], [4] also discussed combining DDP with an Augmented Lagrangian (AL) approach; [8] updated the Lagrange multipliers via forward/backward passes, while [18], [4] utilized schemes from the standard Powell-Hestenes-Rockafellar (PHR) methodology [17] with first-order approximations of the Hessians.

In this paper we build upon the works in [8, 21, 18] to develop a state- and control-constrained version of DDP in discrete time. Specifically, we extend [8, 21] by introducing a slack variable formulation into Bellman’s principle, and thus avoid assumptions regarding the active constraints of the problem. Moreover, we propose an Augmented Lagrangian-inspired algorithm, by considering a set of penalty functions that preserves smoothness of the transformed objective function. This property was not satisfied in [18], but is required to establish the convergence properties of DDP [11]. These two methodologies can be used separately, or be properly combined for improved numerical performance.

We will save the in-depth discussion about technical differ-

ences between our methods and previous papers for subsequent sections. Nevertheless, we note that a comparison among different constrained optimization methods on various simulated scenarios will be provided, which will highlight the efficiency and generalizability of our approach; something which has been lacking from previous DDP-related schemes. To the best of the authors' knowledge, such an extensive experimental study on constrained trajectory optimization has not been conducted in the past. We believe that the current work is a key step towards the development of a numerically robust, constrained version of Differential Dynamic Programming, and opens up multiple directions for research and further improvements.

The remaining of this paper is organized as follows: Section II gives some basics on unconstrained DDP and constrained optimization theory. In Section III we explain our KKT-based DDP algorithm with slack variables (S-KKT), while Section IV discusses our AL-inspired method, as well as a combination thereof. Numerical experiments and in-depth comparisons between our methodologies and previous implementations are provided in Section V. Section VI concludes the paper and discusses possible extensions of the current work.

II. PRELIMINARIES

A. Unconstrained Differential Dynamic Programming

We will briefly cover here the derivation and implementation of Differential Dynamic Programming (DDP). More details can be found in [5, 10].

Consider the discrete-time optimal control problem

$$\begin{aligned} \min_{\mathbf{U}} J(\mathbf{X}, \mathbf{U}) &= \min_{\mathbf{U}} \left[\sum_{k=0}^{N-1} l(\mathbf{x}_k, \mathbf{u}_k) + \phi(\mathbf{x}_N) \right] \\ \text{subject to: } \mathbf{x}_{k+1} &= \mathbf{f}(\mathbf{x}_k, \mathbf{u}_k), \quad k = 0, \dots, N-1. \end{aligned} \quad (1)$$

where $\mathbf{x}_k \in \mathbb{R}^n$, $\mathbf{u}_k \in \mathbb{R}^m$ denote the state and control input of the system at time instant t_k , respectively, and $\mathbf{f} : \mathbb{R}^n \times \mathbb{R}^m \rightarrow \mathbb{R}^n$ corresponds to the transition dynamics function. The scalar-valued functions $l(\cdot, \cdot)$, $\phi(\cdot)$, $J(\cdot)$ denote the running, terminal and total cost of the problem, respectively. We also let $\mathbf{X} := (\mathbf{x}_0^\top, \dots, \mathbf{x}_N^\top)$, $\mathbf{U} := (\mathbf{u}_0^\top, \dots, \mathbf{u}_{N-1}^\top)$ be the state/control sequences over the horizon N .

Of paramount importance is the concept of the *value function*, which represents the minimum cost-to-go at each state and time. It is defined as:

$$V_k(\mathbf{x}_k) := \min_{\mathbf{u}_k} J(\mathbf{X}, \mathbf{U}). \quad (2)$$

Based on this, *Bellman's principle of optimality* gives the following rule:

$$V_k(\mathbf{x}_k) = \min_{\mathbf{u}_k} [l(\mathbf{x}_k, \mathbf{u}_k) + V_{k+1}(\mathbf{x}_{k+1})]. \quad (3)$$

DDP finds local solutions to (1) by expanding both sides of (3) about given nominal trajectories, $\bar{\mathbf{X}}$, $\bar{\mathbf{U}}$. Specifically, let us define the Q function as the argument of min on the right-hand-side of (3):

$$Q_k(\mathbf{x}_k, \mathbf{u}_k) = l(\mathbf{x}_k, \mathbf{u}_k) + V_{k+1}(\mathbf{x}_{k+1}). \quad (4)$$

We now proceed by taking quadratic expansions of Q_k about $\bar{\mathbf{X}}$, $\bar{\mathbf{U}}$. According to (4) and an additional expansion of $\mathbf{x}_{k+1} = \mathbf{f}(\mathbf{x}_k, \mathbf{u}_k)$, this will give

$$\begin{aligned} Q_k(\mathbf{x}_k, \mathbf{u}_k) &\approx Q_k + Q_{\mathbf{x},k}^\top \delta \mathbf{x}_k + Q_{\mathbf{u},k}^\top \delta \mathbf{u}_k + \\ &\quad \frac{1}{2} (\delta \mathbf{x}_k^\top Q_{\mathbf{x}\mathbf{x},k} \delta \mathbf{x}_k + 2 \delta \mathbf{x}_k^\top Q_{\mathbf{x}\mathbf{u},k} \delta \mathbf{u}_k + \delta \mathbf{u}_k^\top Q_{\mathbf{u}\mathbf{u},k} \delta \mathbf{u}_k), \end{aligned}$$

with

$$\begin{aligned} Q_{\mathbf{x}\mathbf{x},k} &= l_{\mathbf{x}\mathbf{x}} + \mathbf{f}_x^\top V_{\mathbf{x},k+1} \mathbf{f}_x, \quad Q_{\mathbf{x},k} = l_x + \mathbf{f}_x^\top V_{\mathbf{x},k+1} \\ Q_{\mathbf{u}\mathbf{u},k} &= l_{\mathbf{u}\mathbf{u}} + \mathbf{f}_u^\top V_{\mathbf{x},k+1} \mathbf{f}_u, \quad Q_{\mathbf{u},k} = l_u + \mathbf{f}_u^\top V_{\mathbf{x},k+1} \\ Q_{\mathbf{x}\mathbf{u},k} &= l_{\mathbf{x}\mathbf{u}} + \mathbf{f}_x^\top V_{\mathbf{x},k+1} \mathbf{f}_u. \end{aligned} \quad (5)$$

Here $\delta \mathbf{x}_k := \mathbf{x}_k - \bar{\mathbf{x}}_k$, $\delta \mathbf{u}_k := \mathbf{u}_k - \bar{\mathbf{u}}_k$ are deviations about the nominal sequences. It is also implied that the Q functions above are evaluated on $\bar{\mathbf{X}}$, $\bar{\mathbf{U}}$.

After plugging (5) into (3), we can explicitly optimize with respect to $\delta \mathbf{u}$ and compute the locally optimal control deviations. These will be given by

$$\begin{aligned} \delta \mathbf{u}_k^* &= \mathbf{k}_k + \mathbf{K}_k \delta \mathbf{x}_k, \\ \text{with } \mathbf{k}_k &:= -Q_{\mathbf{u}\mathbf{u},k}^{-1} Q_{\mathbf{u}}, \quad \mathbf{K}_k = -Q_{\mathbf{u}\mathbf{u},k}^{-1} Q_{\mathbf{x}\mathbf{u},k}. \end{aligned} \quad (6)$$

Finally, observe that $\delta \mathbf{u}^*$ requires knowledge of the value function on the nominal rollout. To this end, V_k will be quadratically expanded and will be plugged along with $\delta \mathbf{u}_k^*$ into (3) to give:

$$\begin{aligned} V_{\mathbf{x},k} &= Q_{\mathbf{x},k} - Q_{\mathbf{x}\mathbf{u},k} Q_{\mathbf{u}\mathbf{u},k}^{-1} Q_{\mathbf{u},k} \\ V_{\mathbf{x}\mathbf{x},k} &= Q_{\mathbf{x}\mathbf{x},k} - Q_{\mathbf{x}\mathbf{u},k} Q_{\mathbf{u}\mathbf{u},k}^{-1} Q_{\mathbf{x}\mathbf{u},k}. \end{aligned} \quad (7)$$

The equations above are propagated backwards in time, since at the final horizon the value function equals the terminal cost. After the backward pass is complete, a new state-control sequence is determined in a forward pass, and this trajectory is then treated as the new nominal trajectory for the next iteration. The procedure is then repeated until certain convergence criteria are satisfied.

To ensure convergence, $Q_{\mathbf{u}\mathbf{u}}$ must be regularized, when its positive definiteness cannot be guaranteed [11]. Typically, line-search on $\delta \mathbf{u}^*$ is also performed with respect to the total cost in the forward pass. We finally note that in this paper we consider only first-order expansions of the dynamics as in [10], which tends to be less computationally expensive and more numerically stable than using second-order terms.

B. Constrained optimization theory

We present here preliminaries on constrained optimization. Due to space limitations, we only consider inequality constraints, though similar results hold for equality constraints.

1) *KKT conditions*: Consider the optimization problem

$$\min_{\mathbf{x}} h(\mathbf{x}) \quad (8)$$

$$\text{subject to } \mathbf{g}(\mathbf{x}) \leq \mathbf{0},$$

where $\mathbf{g} = (g_1(\mathbf{x}), \dots, g_w(\mathbf{x}))^\top$ is a vector of w constraints. The *Lagrangian* is defined as follows:

$$L = h(\mathbf{x}) + \boldsymbol{\lambda}^\top \mathbf{g}(\mathbf{x}), \quad (9)$$

for a real vector $\lambda \in \mathbb{R}^w$. The *Karush–Kuhn–Tucker* (KKT) conditions are necessary optimality conditions for problems of the type (8), and state that a local solution must satisfy [17, Section 12]

$$\frac{\partial L}{\partial \mathbf{x}} = \frac{\partial h(\mathbf{x})}{\partial \mathbf{x}} + \frac{\partial \mathbf{g}(\mathbf{x})^\top}{\partial \mathbf{x}} \lambda = 0$$

$$g_i(\mathbf{x}) \leq 0, \quad \lambda_i \geq 0, \quad \text{and} \quad \lambda_i g_i(\mathbf{x}) = 0, \quad \forall i, \quad (10)$$

where λ now corresponds to the *Lagrange multipliers*. For this result, we need to assume differentiability of f and \mathbf{g} , as well as linear independence of the gradients of active constraints.

2) *Augmented Lagrangian*: Let us define the Augmented Lagrangian function corresponding to (8) as [2, 17]

$$L_A(\mathbf{x}, \lambda, \mu) := h(\mathbf{x}) + \sum_i \mathcal{P}(g_i(\mathbf{x}), \lambda_i, \mu_i), \quad (11)$$

where λ, μ correspond to the Lagrange multipliers and penalty parameters respectively, while $\mathcal{P}(\cdot)$ is the penalty function for inequalities. When $\mathcal{P}(\cdot)$ satisfies certain properties, it can be shown that minimization of (11) can give a solution to (8), under mild assumptions [2].

Loosely speaking, the corresponding optimization process can be divided into an inner and outer loop. In the inner loop, a local minimizer is found for (11) by an unconstrained optimization methodology. At the outer loop, the Lagrange multipliers are updated as: $\lambda_i \leftarrow \mathcal{P}'(g_i, \lambda_i, \mu_i)$, where $\mathcal{P}'(y, \lambda, \mu) := \frac{\partial}{\partial y} \mathcal{P}(y, \lambda, \mu)$. Moreover, the penalty parameters are increased monotonically, when constraint improvement is not satisfactory.

The most popular Augmented Lagrangian algorithm uses the penalty function $P(y, \lambda, \mu) = \frac{1}{2\mu} (\max(0, \lambda + \mu y)^2 - \lambda^2)$ and is known as the Powell-Hestenes-Rockafellar (PHR) method [17]. Despite its success, one key drawback is that the objective function of each subproblem is not twice differentiable, which may cause numerical instabilities when used within second-order algorithms [2].

For completeness, we give the required properties for \mathcal{P} in the appendix, and refer the interested reader to [17, Section 17] and [2].

III. CONSTRAINED DDP USING KKT CONDITIONS AND SLACK VARIABLES

We will henceforth focus on the constrained optimal control problem:

$$\min_{\mathbf{U}} J(\mathbf{X}, \mathbf{U}) = \min_{\mathbf{U}} \left[\sum_{k=0}^{N-1} l(\mathbf{x}_k, \mathbf{u}_k) + \phi(\mathbf{x}_N) \right]$$

$$\text{subject to: } \mathbf{x}_{k+1} = \mathbf{f}(\mathbf{x}_k, \mathbf{u}_k), \quad g_{i,k}(\mathbf{x}_k, \mathbf{u}_k) \leq 0, \quad (12)$$

$$k = 0, \dots, N-1, \quad i = 1, \dots, w.$$

Note that we did not include equality constraints above only for compactness. Our results can be readily extended to this case as well.

A. Backward Pass

Similar to normal unconstrained DDP, the backward pass operates on quadratic approximations of the Q functions about the nominal rollouts (see eqs. (4), (5), (3)). For the constrained case, we can write this as:

$$\min_{\delta \mathbf{u}_k} Q_k(\delta \mathbf{x}_k, \delta \mathbf{u}_k) \quad (13)$$

$$\text{subject to} \quad \tilde{\mathbf{g}}_k(\bar{\mathbf{x}}_k + \delta \mathbf{x}_k, \bar{\mathbf{u}}_k + \delta \mathbf{u}_k) \leq 0.$$

$\tilde{\mathbf{g}}_k$ above is associated with the constraints influenced directly by states and controls at time instance t_k . We will discuss later the selection of such constraints.

We proceed by linearizing the constraints, as well as incorporating the approximate Q function from (5). We have

$$\tilde{\mathbf{g}}_k(\bar{\mathbf{x}}_k + \delta \mathbf{x}_k, \bar{\mathbf{u}}_k + \delta \mathbf{u}_k) \quad (14)$$

$$\approx \tilde{\mathbf{g}}_k(\bar{\mathbf{x}}_k, \bar{\mathbf{u}}_k) + \underbrace{\tilde{\mathbf{g}}_{\mathbf{u}}(\bar{\mathbf{x}}_k, \bar{\mathbf{u}}_k)}_{\mathbf{C}_k} \delta \mathbf{u}_k + \underbrace{\tilde{\mathbf{g}}_{\mathbf{x}}(\bar{\mathbf{x}}_k, \bar{\mathbf{u}}_k)}_{\mathbf{D}_k} \delta \mathbf{x}_k$$

Now, for the approximate problem of (13), the necessary optimality conditions from section II-B1 will read as:

$$Q_{\mathbf{u}\mathbf{u}} \delta \mathbf{u}_k + Q_{\mathbf{u}} + Q_{\mathbf{u}\mathbf{x}} \delta \mathbf{x}_k + \mathbf{C}^\top \lambda_k = \mathbf{0} \quad (15)$$

$$\tilde{g}_i(\mathbf{x}_k) \leq 0, \quad \lambda_{i,k} \geq 0, \quad \text{and} \quad \lambda_{i,k} \tilde{g}_i = 0 \quad (16)$$

where we have dropped the time index on the constraints and Q derivatives for simplicity.

We will now rewrite the above conditions by considering a set of slack variables, such that $s_i + g_i = 0$ and $s_i \geq 0$. Hence, eq. (16) becomes

$$s_{i,k} \geq 0, \quad \lambda_{i,k} \geq 0, \quad s_{i,k} \lambda_{i,k} = 0. \quad (17)$$

To proceed, we will consider perturbations of the slack variables and Lagrange multipliers about their (given) nominal values. Hence we obtain

$$Q_{\mathbf{u}\mathbf{u}} \delta \mathbf{u}_k + Q_{\mathbf{u}} + Q_{\mathbf{u}\mathbf{x}} \delta \mathbf{x}_k + \mathbf{C}_k^\top (\bar{\lambda}_k + \delta \lambda_k) = \mathbf{0} \quad (18)$$

$$(\bar{s}_{i,k} + \delta s_{i,k})(\bar{\lambda}_{i,k} + \delta \lambda_{i,k}) = 0 \quad (19)$$

By omitting the second-order terms, we get

$$\mathbf{S} \bar{\lambda} + \Lambda \delta s_k + \mathbf{S} \delta \lambda_k = \mathbf{0} \quad (20)$$

$$\text{where } \Lambda := \text{diag}(\bar{\lambda}_{i,k}), \quad \mathbf{S} := \text{diag}(\bar{s}_{i,k})$$

Moreover, the slack formulation of the inequality constraints will give

$$\mathbf{S} \mathbf{e} + \delta s_k + \tilde{\mathbf{g}}(\bar{\mathbf{x}}_k, \bar{\mathbf{u}}_k) + \mathbf{C} \delta \mathbf{u}_k + \mathbf{D} \delta \mathbf{x}_k = \mathbf{0} \quad (21)$$

$$\text{where } \mathbf{e} = (1, \dots, 1)$$

Overall, the obtained KKT system can be written in matrix form as

$$\begin{bmatrix} Q_{\mathbf{u}\mathbf{u}} & \mathbf{0} & \mathbf{C}^\top \\ \mathbf{0} & \Lambda & \mathbf{S} \\ \mathbf{C} & \mathbf{I} & \mathbf{0} \end{bmatrix} \begin{bmatrix} \delta \mathbf{u}_k \\ \delta s_k \\ \delta \lambda_k \end{bmatrix} = \begin{bmatrix} -Q_{\mathbf{u}\mathbf{x}} \delta \mathbf{x}_k - Q_{\mathbf{u}} - \mathbf{C}^\top \bar{\lambda}_k \\ -\mathbf{S} \bar{\lambda}_k + \mu_k \sigma_k \mathbf{e} \\ -\mathbf{D} \delta \mathbf{x}_k - \tilde{\mathbf{g}}(\bar{\mathbf{x}}_k, \bar{\mathbf{u}}_k) - \mathbf{S} \mathbf{e} \end{bmatrix} \quad (22)$$

$$\text{with } s_{i,k} \geq 0, \quad \lambda_{i,k} \geq 0.$$

We optimize this system using primal-dual interior point method [17, chapter 18]. $\bar{\lambda}$ is initialized as $\bar{\lambda} = \mathbf{e}$ ($\mathbf{\Lambda} = \mathbf{I}$) since *Lagrange multipliers* are required to be positive. For slack variables s , they are initialized as

$$\bar{s}_{k,i} = \max(-g_i, \epsilon), \quad (23)$$

where ϵ is a small positive number to keep s_i positive and numerically stable. We used $\epsilon = 10^{-4}$.

In the second row of the right hand side of (22), we introduced duality measure:

$$\mu_k = \bar{s}_k^\top \bar{\lambda}_k / w. \quad (24)$$

It is known that if we use the pure Newton direction obtained by $\mu = 0$, we can take only a small step α before violating $s^\top \lambda \geq 0$. To make the direction less aggressive, and the optimization process more effective we reduce $s_i \lambda_i$ to a certain value based on the average value of elementwise product $s_i \lambda_i$, instead of zero. Note that μ is an average value of $s_i \lambda_i$ and μ must converge to zero over the optimization process. We satisfy this requirement by multiplying σ ($0 < \sigma < 1$) [17, Chapter 19].

σ is given by:

$$\sigma_k = 0.1 \min(0.05 \frac{1 - \xi_k}{\xi_k}, 2)^3 \quad (25)$$

$$\text{where } \xi_k = \frac{\min_i(s_{i,k} \lambda_{i,k})}{\mu_k}. \quad (26)$$

Our goal is to solve the above system analytically, which, as we will find, requires the inversion of \mathbf{S} and $\mathbf{\Lambda}$. It might be the case, however, that these matrices are close to being singular; for example, elements of \mathbf{S} will be close to zero when the corresponding constraints approach their boundaries. To tackle this problem we will perform the following change of variables

$$\delta \mathbf{p}_k := \mathbf{S}^{-1} \delta \mathbf{s}_k, \quad \delta \mathbf{q}_k := \mathbf{\Lambda}^{-1} \delta \mathbf{\lambda}_k. \quad (27)$$

Then the new KKT system can be obtained as

$$\begin{bmatrix} Q_{uu} & \mathbf{0} & C^\top \mathbf{\Lambda} \\ \mathbf{0} & \mathbf{\Lambda} \mathbf{S} & \mathbf{S} \mathbf{\Lambda} \\ \mathbf{\Lambda} \mathbf{C} & \mathbf{\Lambda} \mathbf{S} & \mathbf{0} \end{bmatrix} \begin{bmatrix} \delta \mathbf{u}_k \\ \delta \mathbf{p}_k \\ \delta \mathbf{q}_k \end{bmatrix} = \begin{bmatrix} -Q_{ux} \delta \mathbf{x}_k - Q_u - C_k^\top \bar{\lambda}_k \\ -\mathbf{S} \bar{\lambda}_k + \mu_k \sigma_k \mathbf{e} \\ -\mathbf{\Lambda} (D_k \delta \mathbf{x}_k + \tilde{\mathbf{g}}(\bar{\mathbf{x}}_k, \bar{\mathbf{u}}_k) + \mathbf{S} \mathbf{e}) \end{bmatrix} = \begin{bmatrix} \mathbf{a} \\ \mathbf{b} \\ \mathbf{\Lambda} \mathbf{d} \end{bmatrix} \quad (28)$$

s.t. $s_{i,k} \geq 0, \quad \lambda_{i,k} \geq 0.$

We can now avoid singularity issues, since $\mathbf{\Lambda} \mathbf{S} \rightarrow \mu_k \sigma_k$ (instead of 0) with our new formulation.

Now notice that in the backward pass of DDP, we do not have $\delta \mathbf{x}$. Hence, our strategy will be to first solve the KKT system on the nominal rollout by substituting $\delta \mathbf{x} = \mathbf{0}$, and then use our optimal values of s and λ as our \bar{s} and $\bar{\lambda}$ for the next KKT iteration.

An analytical solution for this case can be obtained by algebraic manipulations, which we state below:

$$\delta \mathbf{q} = \mathbf{M}(\mathbf{E} \mathbf{Q}_{uu}^{-1} \mathbf{a} - \mathbf{\Lambda} \mathbf{d} + \mathbf{b}) \quad (29)$$

$$\delta \mathbf{p} = \mathbf{F}^{-1}(\mathbf{b} - \mathbf{F} \delta \mathbf{q}) \quad (30)$$

$$\delta \mathbf{u} = \mathbf{a} - \mathbf{E}^\top \delta \mathbf{q} \quad (31)$$

$$\text{where } \mathbf{M} = (\mathbf{E} \mathbf{Q}_{uu}^{-1} \mathbf{E}^\top + \mathbf{F})^{-1} \quad (32)$$

$$\mathbf{E} = \mathbf{\Lambda} \mathbf{C}, \quad \mathbf{F} = \mathbf{\Lambda} \mathbf{S}.$$

We will next update \bar{s} and $\bar{\lambda}$ by

$$\bar{s}_k = \bar{s}_k + \alpha \delta \mathbf{s}_k, \quad \bar{\lambda}_k = \bar{\lambda}_k + \alpha \delta \mathbf{\lambda}_k. \quad (33)$$

The step size α must be determined to keep s_k and λ_k non-negative. The following strategy is also used in interior point methods [17, Chapter 16].

$$\alpha = \min(\alpha_s, \alpha_\lambda) \quad (34)$$

$$\alpha_s = \min_{\delta s_{i,k}^k < 0} (1, -\zeta \frac{s_{i,k}}{\delta s_{i,k}}), \quad \alpha_\lambda = \min_{\delta \lambda_{i,k} < 0} (1, -\zeta \frac{\lambda_{i,k}}{\delta \lambda_{i,k}}) \quad (35)$$

$$\text{where } 0.9 \leq \zeta < 1.$$

When there are no negative elements in $\delta \mathbf{s}$ or $\delta \mathbf{\lambda}$, the corresponding step sizes are taken to be $\alpha_s = 1$ and $\alpha_\lambda = 1$. Using this step size, we also update the linearized constraint function and the Q function. For convenience, we write the new $\bar{\mathbf{u}}_k$ as $\bar{\mathbf{u}}_k + \alpha \delta \mathbf{u}_k^{j-1}$. $j-1$ implies that $\delta \mathbf{u}$ is from one iteration before. Then the updated constraint function on the nominal trajectory ($\delta \mathbf{x} = \mathbf{0}$) is:

$$\begin{aligned} & \tilde{\mathbf{g}}(\bar{\mathbf{u}}_k + \alpha \delta \mathbf{u}_k^{j-1} + \delta \mathbf{u}_k) \\ & \approx \tilde{\mathbf{g}}(\bar{\mathbf{u}}_k) + \tilde{\mathbf{g}}_u(\alpha \delta \mathbf{u}_k^{j-1} + \delta \mathbf{u}_k) \\ & = (\tilde{\mathbf{g}}(\bar{\mathbf{u}}_k) + \mathbf{C}_k \alpha \delta \mathbf{u}_k^{j-1}) + \mathbf{C}_k \delta \mathbf{u}_k. \end{aligned} \quad (36)$$

Therefore the updated nominal constraint function is

$$\mathbf{g}(\bar{\mathbf{u}}_k) = \mathbf{g}(\bar{\mathbf{u}}_k) + \mathbf{C}_k \alpha \delta \mathbf{u}_k^{j-1}. \quad (37)$$

For Q function, we expand them around nominal trajectory considering small perturbation.

$$\begin{aligned} & Q(\bar{\mathbf{u}}_k + \alpha \delta \mathbf{u}_k^{j-1} + \delta \mathbf{u}_k) \\ & \approx \frac{1}{2}(\alpha \delta \mathbf{u}_k^{j-1} + \delta \mathbf{u}_k)^\top Q_{uu}(\alpha \delta \mathbf{u}_k^{j-1} + \delta \mathbf{u}_k) \\ & \quad + Q_u^\top(\alpha \delta \mathbf{u}_k^{j-1} + \delta \mathbf{u}_k). \end{aligned} \quad (38)$$

Using this new Q function we construct *Lagrangian* as,

$$\begin{aligned} L = & \frac{1}{2}(\alpha \delta \mathbf{u}_k^{j-1} + \delta \mathbf{u}_k)^\top Q_{uu}(\alpha \delta \mathbf{u}_k^{j-1} + \delta \mathbf{u}_k) \\ & + Q_u^\top(\alpha \delta \mathbf{u}_k^{j-1} + \delta \mathbf{u}_k) + \lambda^\top (\tilde{\mathbf{g}}(\bar{\mathbf{u}}_k) + \mathbf{C}_k \alpha \delta \mathbf{u}_k^{j-1} + \mathbf{C}_k \delta \mathbf{u}_k). \end{aligned} \quad (39)$$

From KKT condition $\frac{\partial L}{\partial \delta \mathbf{u}_k}$, we have

$$Q_{uu}(\delta \mathbf{u}_k + \alpha \delta \mathbf{u}_k^{j-1}) + Q_u + C_k^\top \lambda = \mathbf{0}. \quad (40)$$

Comparing the above equation with (18) on the nominal trajectory ($\delta \mathbf{x}_k = \mathbf{0}$), the new Q_u can be obtained as

$$Q_u = Q_u + \alpha Q_{uu} \delta \mathbf{u}_k^{j-1}. \quad (41)$$

and the KKT system (22) is iteratively solved, updating \bar{s} , $\bar{\lambda}$, and μ_k , until the duality measure μ_k is improved to a certain threshold. In this paper we used 0.01 as the threshold. Finally, using the updated \bar{s}_k and $\bar{\lambda}_k$, we solve the system at the perturbed trajectory ($\delta x \neq 0$) for δu_k :

$$\delta u_k = -Q_{uu}^{-1}[HQ_u + E^T M \Lambda(\tilde{g}(\bar{x}_k, \bar{u}_k) + Se)] - Q_{uu}^{-1}(HQ_{ux} + E^T M \Lambda D)\delta x_k \quad (42)$$

$$\text{where } H = I - E^T M E Q_{uu}^{-1}. \quad (43)$$

The feedforward gain, k , and feedback gain, K , can then be obtained as follows:

$$k = -Q_{uu}^{-1}[HQ_u + E^T M \Lambda(g(\bar{x}_k, \bar{u}_k) + Se)] \quad (44)$$

$$K = -Q_{uu}^{-1}(HQ_{ux} + E^T M \Lambda D) \quad (45)$$

We will finally discuss which constraints \tilde{g} to consider. We assume the full state x is composed of position $x^p \in \mathbb{R}^{n_p}$, a function of state itself, and $x^v \in \mathbb{R}^{n_v}$, a function of state and control: $x = [x^p, x^v]^T$. p implies position, and v implies velocity.

$$x_{k+2}^p = f^p(x_{k+1}), \quad \begin{bmatrix} x_{k+1}^p \\ x_{k+1}^v \end{bmatrix} = \begin{bmatrix} f^p(x_k) \\ f^v(x_k, u_k) \end{bmatrix}. \quad (46)$$

u_k (control at time step k) that we obtain by solving QP does not affect the x_k state at the same time step, but x^p two time steps forward x_{k+2}^p , and x^v one time step forward x_{k+1}^v . This implies that we should solve the QP subject to constraints two time steps forward for x^p , and one time step forward for x^v . We use this fact to resolve the problem when C is zero in our algorithm. If C is zero, feedback and feedforward gains are the same as normal unconstrained DDP, see (33), (43), (44), and (45). First, we divide elements of g_k into function of x^p , x^v , and u_k , and write them as g_k^p , g_k^v , and g_k^c . For g_k^p we propagate two time steps, and for g_k^v one time step forward to make them explicit functions of u_k . Expanded g_{k+2}^p can be calculated using the chain rule:

$$g_{k+2}^p(\bar{x}_k + \delta x_k, \bar{u}_k + \delta u_k) \approx g_{k+2}^p(\bar{x}_k, \bar{u}_k) + \underbrace{\frac{\partial g_{k+2}^p}{\partial x_k}}_{D_k^p} \delta x_k + \underbrace{\frac{\partial g_{k+2}^p}{\partial u_k}}_{C_k^p} \delta u_k \quad (47)$$

where

$$\frac{\partial g_{k+2}^p}{\partial x_k} = \frac{\partial g_{k+2}^p}{\partial x_{k+2}^p} \frac{\partial x_{k+2}^p}{\partial x_{k+1}} \frac{\partial x_{k+1}}{\partial x_k} = \frac{\partial g_{k+2}^p}{\partial x_{k+2}^p} f_{x,k+1}^p f_{x,k} \quad (48)$$

$$\frac{\partial g_{k+2}^p}{\partial u_k} = \frac{\partial g_{k+2}^p}{\partial x_{k+2}^p} \frac{\partial x_{k+2}^p}{\partial x_{k+1}} \frac{\partial x_{k+1}}{\partial u_k} = \frac{\partial g_{k+2}^p}{\partial x_{k+2}^p} f_{x,k+1}^p f_{u,k} \quad (49)$$

g_{k+1}^v is:

$$g_{k+1}^v(\bar{x}_k + \delta x_k, \bar{u}_k + \delta u_k) \approx g_{k+1}^v(\bar{x}_k, \bar{u}_k) + \underbrace{\frac{\partial g_{k+1}^v}{\partial x_k}}_{D_k^v} \delta x_k + \underbrace{\frac{\partial g_{k+1}^v}{\partial u_k}}_{C_k^v} \delta u_k \quad (50)$$

$$\frac{\partial g_{k+1}^v}{\partial x_k} = \frac{\partial g_{k+1}^v}{\partial x_{k+1}} \frac{\partial x_{k+1}}{\partial x_k} = \frac{\partial g_{k+1}^v}{\partial x_{k+1}} f_{x,k} \quad (51)$$

$$\frac{\partial g_{k+1}^v}{\partial u_k} = \frac{\partial g_{k+1}^v}{\partial x_{k+1}} \frac{\partial x_{k+1}}{\partial u_k} = \frac{\partial g_{k+1}^v}{\partial x_{k+1}} f_{u,k} \quad (52)$$

For g^c we use the same expressions as \tilde{g} .

Stacking g , C , and D , we have the linearized constraints

$$g(\bar{x}_k, \bar{u}_k) = \begin{bmatrix} g_{k+2}^p \\ g_{k+1}^v \\ g_k^c \end{bmatrix}, C_k = \begin{bmatrix} C_k^p \\ C_k^v \\ C_k^c \end{bmatrix}, D_k = \begin{bmatrix} D_k^p \\ D_k^v \\ D_k^c \end{bmatrix} \quad (53)$$

Algorithm 1: Backward Pass

- 1: Initialize: $V_N \leftarrow \phi(\bar{x}_N)$
 $V_{x,N} \leftarrow \nabla_x \phi(\bar{x}_N)$, $V_{xx,N} \leftarrow \nabla_{xx} \phi(\bar{x}_N)$
 - 2: **for** $k = N - 1$ to 0 **do**
 - 3: Calculate l , Q , and their derivatives at k
 - 4: Regularize Q_{uu} , Q_{ux} , and Q_{ux} using ν_1 and ν_2
 \bar{s} and $\bar{\lambda}$ process
 - 5: Initialize $\bar{s}_{k,i} = \max(-g_i, \epsilon)$, $\bar{\lambda}_{k,i} = 1$
 - 6: $\mu_0 \leftarrow s^T \lambda / w$
 - 7: **while** $\mu / \mu_0 < 0.01$ **do**
 - 8: Solve KKT system to obtain δu_k , δs_k , and $\delta \lambda_k$
 - 9: Determine step size α
 - 10: Update \bar{u}_k , \bar{s}_k , $\bar{\lambda}_k$, $g(\bar{x}_k, \bar{u}_k)$, and Q_u
 - 11: $\mu \leftarrow \bar{s}_k^T \bar{\lambda}_k / w$
 - 12: **end while**
 - Update gains and value functions
 - 13: $k \leftarrow -Q_{uu}^{-1}[HQ_u + E^T M \Lambda(g(\bar{x}, \bar{u}) + Se)]$
 - 14: $K \leftarrow -Q_{uu}^{-1}(HQ_{ux} + E^T M \Lambda D)$
 - 15: $V_x \leftarrow Q_x + K^T Q_{uu} k + K^T Q_u + Q_{ux}^T k$
 - 16: $V_{xx} \leftarrow Q_{xx} + K^T Q_{uu} K + K^T Q_{ux} + Q_{ux}^T K$
 - 17: **end for**
 - 18: Store Derivatives of Q
-

B. Forward Pass

The following QP problem is solved which takes into account all the constraints to guarantee the updated nominal trajectory is feasible:

$$\arg \min_{\delta u_k} \left[\frac{1}{2} \delta u_k^T Q_{uu} \delta u_k + Q_u^T \delta u_k + \delta u_k^T Q_{ux} \delta x_k \right] \quad (54)$$

$$\text{subject to } g_k(\bar{x}_k + \delta x_k, \bar{u}_k + \delta u_k) \approx g_k(\bar{x}_k, \bar{u}_k) + D_k \delta x_k + C_k \delta u_k \leq 0$$

Note that δu_k is used to obtain x_{k+1} and we already have δx_k . The updated nominal state, $\bar{x}'_k = \bar{x}_k + \delta x_k$, can be used instead of the previous iteration's \bar{x}_k and δx_k . Thus the δx term for \bar{x}'_k in the linearized constraint equation becomes zero and we obtain the following:

$$g_k(\bar{x}'_k, u_k + \delta u_k) = g_k(\bar{x}'_k, u_k) + C_k(\bar{x}'_k, u_k) \delta u_k \leq 0 \quad (55)$$

Again, one or two time step propagation of g shown in backward pass is important, because otherwise C_k might be

Algorithm 2: Algorithm for forward pass

```

1: Calculate  $J_{int} \leftarrow J(\mathbf{X}, \mathbf{U})$ 
2:  $\mathbf{x} \leftarrow \mathbf{x}_0$ 
3:  $\mathbf{X}_{temp} \leftarrow \mathbf{X}, \quad \mathbf{U}_{temp} \leftarrow \mathbf{U}$ 
4: for  $k = 0$  to  $N - 2$  do
5:    $\delta \mathbf{x} \leftarrow \mathbf{x} - \mathbf{x}_k$ 
6:    $\mathbf{x}_{temp,k} \leftarrow \mathbf{x}$ 
   Solve QP:
7:    $\delta \mathbf{u}_k^* = \arg \min [\frac{1}{2} \delta \mathbf{u}_k^T Q_{uu} \delta \mathbf{u}_k + \delta \mathbf{u}_k^T (Q_u + Q_{ux} \delta \mathbf{x}_k)],$ 
   subject to  $\mathbf{g}_k(\mathbf{x}, \mathbf{u}_k) + \mathbf{C}_k(\mathbf{x}, \mathbf{u}_k) \delta \mathbf{u}_k \leq \mathbf{0}$ 
8:    $\mathbf{u}_{temp,k} = \mathbf{u}_k + \delta \mathbf{u}_k^*$ 
9:    $\mathbf{x} \leftarrow \mathbf{f}(\mathbf{x}, \mathbf{u}_{temp,k})$ 
10: end for
11:  $\delta \mathbf{x} \leftarrow \mathbf{x} - \mathbf{x}_{N-1}$ 
12:  $\mathbf{x}_{temp,N-1} \leftarrow \mathbf{x}$ 
13: while flag = False do
14:   flag = True
   Solve QP:
15:    $\delta \mathbf{u}_{N-1}^* = \arg \min [\frac{1}{2} \delta \mathbf{u}_{N-1}^T Q_{uu} \delta \mathbf{u}_{N-1} +$ 
    $\delta \mathbf{u}_{N-1}^T (Q_u + Q_{ux} \delta \mathbf{x}_{N-1})],$  subject to  $|\mathbf{u}_{N-1}| \leq \Delta$ 
   Update  $\mathbf{x}, \mathbf{u}$  and Check Feasibility of QP
16:    $\mathbf{u}_{temp,N-1} = \mathbf{u}_{N-1} + \delta \mathbf{u}_{N-1}^*$ 
17:    $\mathbf{x}_{temp,N} \leftarrow \mathbf{f}(\mathbf{x}, \mathbf{u}_{temp,N-1})$ 
18:   if any  $\mathbf{g}(\mathbf{x}_{temp,N}) > 0$  then
19:     flag = False
20:      $\Delta \leftarrow \eta \Delta$ 
21:   break
22:   end if
23: end while
24: Calculate  $J_{temp} \leftarrow J(\mathbf{X}_{temp}, \mathbf{U}_{temp})$ 
25: if  $J_{temp} < J_{int}$  then
26:    $\mathbf{X} \leftarrow \mathbf{X}_{temp}, \mathbf{U} \leftarrow \mathbf{U}_{temp}$ 
27:   Decrease  $\nu_1$  and  $\nu_2$ .
28: else
29:   Increase  $\nu_1$  and  $\nu_2$ .
30: end if
```

zero, and \mathbf{u}_k does not show up in the linearized constraint. At time step N , constraints \mathbf{g}_{N+2}^p are not available because the time horizon ends at time step $N + 1$. Hence, we solve the QP under box constraints

$$-\Delta \leq \delta \mathbf{u}_N \leq \Delta \quad (56)$$

Δ is a vector of an adaptive trust region initialized by a relatively large positive value. If the solution is not feasible, Δ is made to be smaller by

$$\Delta = \eta \Delta, \quad \text{where } 0 < \eta < 1 \quad (57)$$

This makes the new trajectory closer to the trajectory one iteration before, which is feasible. The trust region is made smaller repeatedly until the solution of the QP becomes feasible.

C. Regularization

In DDP, regularization plays a big role and highly affects the convergence. We use the regularization scheme and scheduling technique proposed in [19].

$$Q_{xx} = l_{xx} + \mathbf{f}_x^T (V'_{xx} + \nu_1 \mathbf{I}_n) \mathbf{f}_x \quad (58)$$

$$Q_{ux} = l_{ux} + \mathbf{f}_u^T (V'_{xx} + \nu_1 \mathbf{I}_n) \mathbf{f}_x \quad (59)$$

$$Q_{uu} = l_{uu} + \mathbf{f}_u^T (V'_{xx} + \nu_1 \mathbf{I}_n) \mathbf{B} + \nu_2 \mathbf{I}_m \quad (60)$$

These regularized derivatives are used to calculate gains \mathbf{k} and \mathbf{K} , and instead of using (7) we update the value function as follows:

$$V_x = Q_x + \mathbf{K}^T Q_{uu} \mathbf{k} + \mathbf{K}^T Q_u + Q_{ux}^T \mathbf{k} \quad (61)$$

$$V_{xx} = Q_{xx} + \mathbf{K}^T Q_{uu} \mathbf{K} + \mathbf{K}^T Q_{ux} + Q_{ux}^T \mathbf{K} \quad (62)$$

Both ν_1 and ν_2 are positive values. ν_1 makes the new trajectory closer to the previous one, while ν_2 makes the control step conservative and makes Q_{uu} positive definite.

IV. CONSTRAINED DDP WITH AUGMENTED LAGRANGIAN METHODS

A. AL-DDP and penalty function

Here, we will be using the Augmented Lagrangian approach to extend DDP for solving (12). We call this technique AL-DDP. The main idea is to observe that *partial elimination of constraints* can be used on the inequality constraints \mathbf{g} of (12). This means that the penalty function \mathcal{P} from section II-B2 can only be applied to the inequality state constraints, while the dynamics are implicitly satisfied due to DDP's problem formulation. We will thus be considering the following problem

$$\min_{\mathbf{U}} \left[\underbrace{J(\mathbf{X}, \mathbf{U}) + \sum_{i,k} \mathcal{P}(\lambda_i^k, \mu_i^k, g_{i,k}(\mathbf{x}_k, \mathbf{u}_k))}_{L_A} \right]$$

s.t. $\mathbf{x}_{k+1} = \mathbf{f}(\mathbf{x}_k, \mathbf{u}_k), \quad \mathbf{x}^0 = \bar{\mathbf{x}}^0, \quad k = 0, 1, \dots, H-1, \quad (63)$

where λ_i^k, μ_i^k denote Lagrange multipliers and penalty parameters respectively. We will thus be using the approach discussed in section II-B2, using specifically unconstrained DDP to optimize (63), followed by an update on the Lagrange multipliers and the penalty parameters.

Since DDP requires $L_A(\cdot)$ to be twice differentiable, we selected the penalty function as

$$\mathcal{P}(\lambda_{i,k}, \mu_{i,k}, g_{i,k}(\mathbf{x}_k)) = \frac{(\lambda_{i,k})^2}{\mu_{i,k}} \phi\left(\frac{\mu_{i,k}}{\lambda_{i,k}} g_{i,k}(\mathbf{x}_k)\right),$$

with

$$\phi(t) := \begin{cases} \frac{1}{2}t^2 + t, & t \geq -\frac{1}{2} \\ -\frac{1}{4}\log(-2t) - \frac{3}{8}, & \text{otherwise,} \end{cases}$$

which can be viewed as a smooth approximation to the Powell-Hestenes-Rockafellar method [2].

B. Combination of AL-DDP and KKT frameworks

The Augmented Lagrangian approach is typically robust to initializations of the algorithm, but displays oscillatory behavior near the (local) solution [2]. This can be readily explained from optimization theory, since Multiplier methods generally converge only linearly [2].

The idea here is to combine the two approaches: We begin by using the AL-DDP formulation until a pre-specified precision of the cost and constraints, and subsequently switch to the KKT-based approach of section III. If sufficient improvement is not observed within a few iterations, we switch back to the Augmented Lagrangian method, and reduce the aforementioned tolerances for the “switching” mechanism. We also have one more reason for the combination. By applying the control limited DDP technique [20] in the backward pass of the Augmented Lagrangian method, we can handle the control limits as a hard box constraint. In the control limited DDP method, the feedforward gain k_k is obtained as

$$k_k = \arg \min_{\delta u_k} \frac{1}{2} \delta u_k^T Q_{uu} \delta u_k + \delta u_k^T Q_{u} \quad (64)$$

$$u_l \leq u_k + \delta u_k \leq u_u,$$

where u_l is the lower and u_u is the upper limit of control. For the feedback gain K_k , corresponding rows to the active control limits are set to be zero. As we will discuss in Section III, our KKT-based method can not handle a situation when state and control constraints conflict with each other. This situation typically happens when initial state is far from desired state and a large control is required. By providing a good initial trajectory from AL for the KKT-based method, our method can successfully handle both state and control constraints.

V. RESULTS

In this section we provide simulation results and comparisons between our method and prior work. We call our method “S-KKT” named after the slack variable and KKT conditions. We also test a slightly different version from S-KKT, in which we use the active set method [12] instead of slack variables, but still use one and two time step forward expansion of the constraint function. More precisely, in this method, constraints are took into account only when they are close to active, and they are linerarized under an assumption that active constraints in current iteration remains to be active in next iteration, that is

$$g(\bar{x}_k + \delta x_k, \bar{u}_k + \delta u_k) = g(\bar{x}_k, \bar{u}_k) \approx 0. \quad (65)$$

Using this assumption in (14), constraints are written as

$$C_k \delta u_k + D_k \delta x_k = 0, \quad (66)$$

and QP is solved under this equality constraints instead of (55). The purpose of showing this algorithm here is to see the effect of slack variables and the assumption in (65). We call this method the “active set method”. We evaluate these methods and compare them with the former method [21]. The next step is to combined our methods with other optimization algorithms and evaluate the performance.

A. S-KKT

We evaluate our constrained DDP algorithms in two different systems, a simplified 2D car and a quadrotor.

1) *2D car*: We consider a 2D car following with dynamics give by the expression below [21]:

$$\begin{bmatrix} x_{k+1} \\ y_{k+1} \\ \theta_{k+1} \\ v_{k+1} \end{bmatrix} = \begin{bmatrix} x_k + v_k \sin \theta_k \Delta t \\ y_k + v_k \cos \theta_k \Delta t \\ \theta_k + u_k^\theta v_k \Delta t \\ v_k + u_k^v \Delta t \end{bmatrix} \quad (67)$$

. The car has state $x = [x, y, \theta, v]^T$, and control u^θ on the steering angle and u^v on the velocity. We consider a reaching task to $x_g = [3, 3, \frac{\pi}{2}, 0]^T$ while avoiding three obstacles. The obstacles are formulated as

$$g_{\text{car}} = \begin{bmatrix} 0.5^2 - (x-1)^2 - (y-1)^2 \\ 0.5^2 - (x-1)^2 - (y-2.5)^2 \\ 0.5^2 - (x-2.5)^2 - (y-2.5)^2 \end{bmatrix} \leq 0. \quad (68)$$

Fig. 1 shows the result of the task starting from several initial points per algorithm. Optimization starts with six different initial points with no control. Fig. 2 shows the result of starting from initial trajectories. From left to right, a feasible trajectory, slightly infeasible trajectory, and close to the optimal trajectory were used as initial trajectories.

In the S-KKT algorithm, as we explained in eq. 23 and Algorithm 1, \bar{s} is initialized by a positive value ϵ . This means that the algorithm regards the initial trajectory feasible even though it is not. We experimentally confirmed that this is fine as long as the violation is small. In fact, this means S-KKT is able to handle initial trajectories that are slightly infeasible, which is something previous constrained DDP algorithms cannot handle.

The procedure of the experiment is as follows. We made several initial trajectories with different amounts of violations by changing the radii of obstacles and used them as initial trajectories of the original problem. In our 2D car setting, original radii of obstacles are 0.5 m. We changed radius to 0.4 and ran the algorithm to get an optimized trajectory. Then, we used this trajectory as an initial trajectory with 0.1 violation for the original problem whose obstacles have 0.5 radii. Our algorithm could successfully handle an initial violation up to 0.3.

Fig. 3 shows the relationship between cost, max. value of constrained function g and iteration initialized with several start points. Fig. 4 shows that of starting with initial trajectories. We specified the number of maximum outer iterations to be 15. The algorithm stops either when the max iteration is reached, when the regularizers are larger than the criteria, or the gradient of objective is very small. Introducing the slack variable in our method makes the trajectory smoother and we obtain the lowest converged cost. Our method could also get out of the prohibited region.

2) *Quadrotor*: We test our algorithm on a quadrotor system [13]. The quadrotor reaches a goal $x_g = [1, 5, 5]^T$ avoiding three obstacles. Fig. 5 shows trajectories starting with four different initial hovering points from three different algorithms,

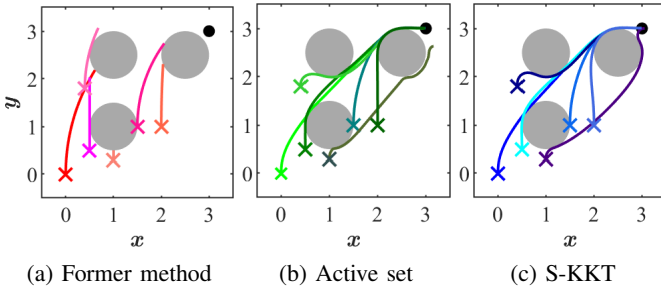


Fig. 1: 2D car trajectories starting from several initial points. Starting points are shown by “x”.

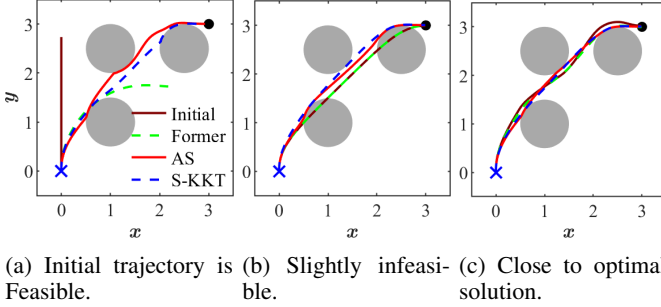


Fig. 2: 2D car trajectories starting from several initial trajectories.

that is, former KKT algorithm, active set method, and S-KKT. And Fig. 6 shows the cost and max. value of the constrained function g . Again, S-KKT has the best performance.

B. Combination of S-KKT and Augmented Lagrangian method

1) *Control constraints*: Because S-KKT can take constraints in consideration only two time steps forward, sometimes state and control constraints conflict with each other. In the 2D car case, for example, a car is trying to reach the target and suddenly finds an obstacle. If the control is not limited, the car can quickly steer to dodge the obstacle. However, if the control is limited, it cannot perform a sudden turn and makes a collision, making the trajectory infeasible. Fig. 7 shows how the control changes over iterations when the control is not limited. In this example, a 2D car starts from a static point $[0, 0, 0, 0]$ with $\mathbf{0}$ initial control and reaches x_g explained in Section V-A1. In early iterations, large control spikes are observed. These spikes get smaller in future iterations, because the high control is penalized in the cost function. We can expect the optimizer to make the control spikes smaller than the arbitrary control limits, but there is no guarantee. Therefore S-KKT cannot explicitly apply control constraints to a trajectory as it is. We solve this problem by combining AL-DDP and S-KKT. Using the control limited DDP technique in the backward pass, AL-DDP can apply control constraints to a trajectory. AL-DDP is very fast for the first few iterations but gets slow when it comes close to the boundary of constraints and sometimes violates the constraints. Usually the trajectory oscillates around the boundary. Whereas S-KKT takes relatively a longer time for one iteration, but can

keep feasibility. Though S-KKT can not handle a problem in which state and control constraints conflict each other. Typically the conflict happens when the initial state is far from the goal state and it needs to be changed a lot. However, given a good initial trajectory, S-KKT is good at pushing it close to boundary as shown in Fig. 2. We feed S-KKT with the output of AL-DDP and optimize it under the expectation that large control is not required. The concept of the combination is shown in Fig. 8. After receiving an optimized trajectory from AL-DDP, S-KKT solves the QP problem in its forward pass shown in eq. (54) with additional box control constraints,

$$\mathbf{u}_l - \bar{\mathbf{u}}_k \leq \delta \mathbf{u}_k \leq \mathbf{u}_u - \bar{\mathbf{u}}_k, \quad (69)$$

If the QP problem is infeasible at time step t_k , we make the control more conservative by multiplying $0 < \eta < 1$ to the box constraints as we do in (57),

$$\eta(\mathbf{u}_l - \bar{\mathbf{u}}_k) \leq \delta \mathbf{u}_k \leq \eta(\mathbf{u}_u - \bar{\mathbf{u}}_k), \quad (70)$$

and resolve the QP problem again from t_0 until the problem can be solved over the entire time horizon. This strategy, making a trajectory closer to a former one until it becomes feasible, is not good when the initial trajectory is far from desired one, and/or large control is required to dodge the obstacles as shown in Fig. 7. In our case, however, thanks to a good initial trajectory from AL-DDP, this strategy fits well with S-KKT.

2) *2D car*: To examine the performance of the combination, we used the same problem setting of the 2D car in Section V-A1, and applied control limit as,

$$-\frac{\pi}{3} \leq u^\theta \leq \frac{\pi}{3}, \quad -6 \leq u^v \leq 6 \quad (71)$$

The results and comparison between unconstrained control case are shown in Fig. 9. The algorithm could successfully handle both state and control constraints.

We observed that when the steering control constraint was too tight, the car could only satisfy the desired angle (see pink trajectory in Fig. 9a). In its control graph in Fig. 9b, we can see that maximum steering control was applied to dodge the obstacle and to reach the goal but it was not enough. As shown in the green trajectory in Fig. 9a, it reached the goal, dodging the first obstacle from the top. Whereas in the control unconstrained case in Fig. 1, it could make a sharp turn and dodge the first obstacle from the bottom. This change can be also seen by comparing Fig. 9b and Fig. 9d. In the constrained case,

C. Performance Analysis

Next we perform a thorough analysis between five algorithms, SQP, S-KKT based DDP, AL-DDP, AL-DDP with SQP, and AL-DDP with S-KKT. The SQP algorithm used in this comparison is the one available through Matlab's Optimization Toolbox. For the rest of the algorithms, we have implemented them ourselves. In the five algorithms, the last two, AL-DDP with SQP and AL-DDP with S-KKT are a

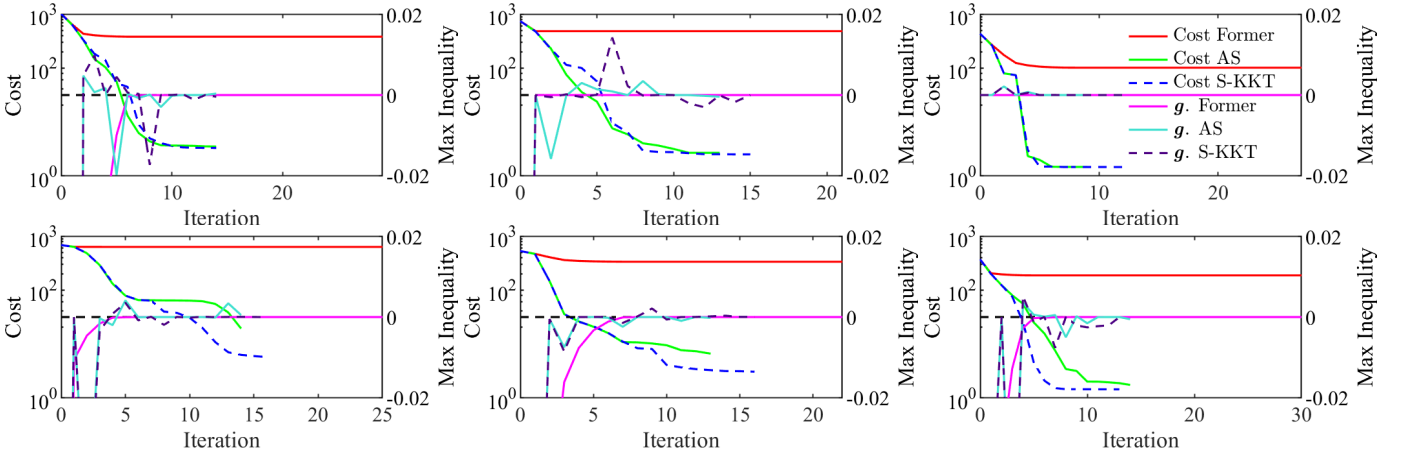


Fig. 3: Cost and max. inequality constraint of 2D car starting from several initial points.

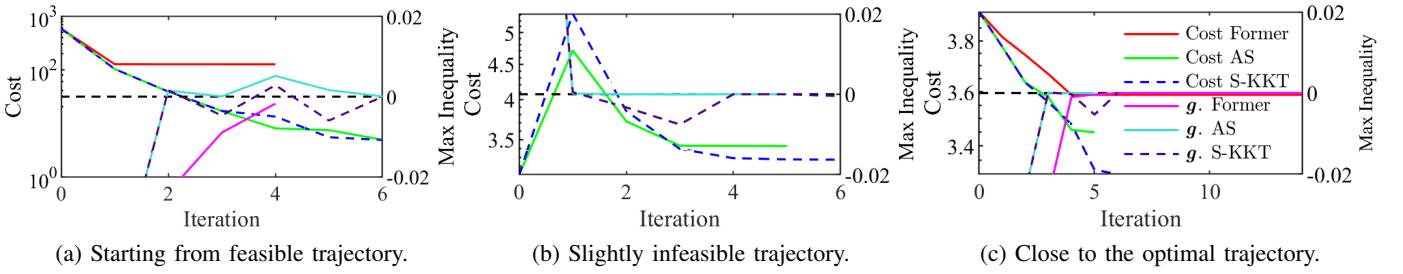


Fig. 4: Cost and max. inequality constraint of 2D car starting from several initial trajectories.

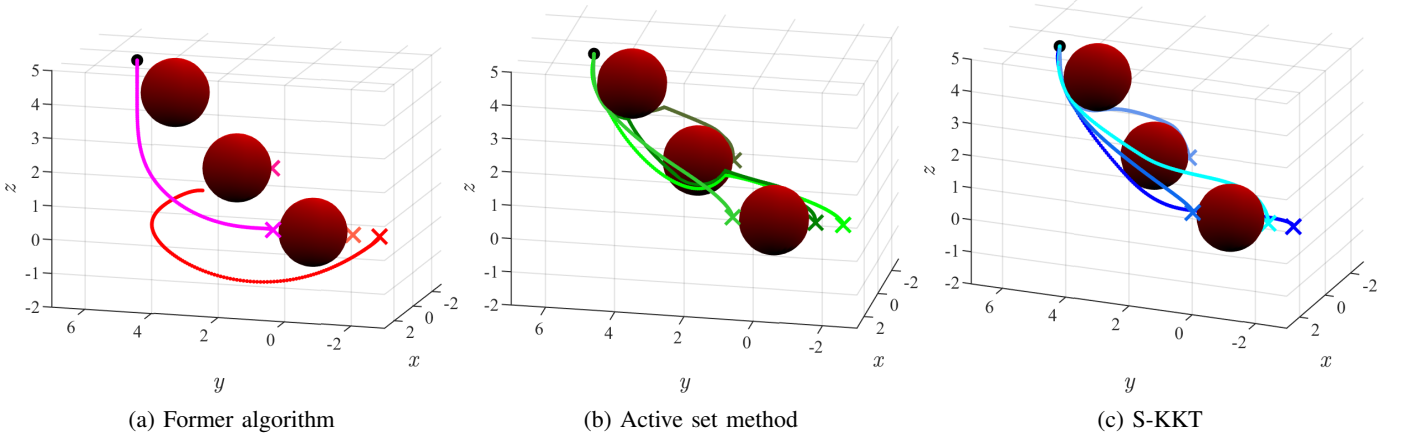


Fig. 5: Trajectories from different algorithms. Starting points are shown by “x”.

combination of two different optimization algorithms. In these two combination methods, the algorithms start optimizing using AL-DDP and switch to SQP or S-KKT as explained in IV-B. We compare the five algorithms in terms of performance metrics, namely cost, time, and feasibility, in three systems, cart pole, 2D car, and quadrotor. We also specify different time horizons for the same examples. Here the time horizon H is the number of time steps and the time step size dt is fixed in each example. Furthermore, we perform experiments with a time budget as well as letting the algorithms run until they have reached the convergence criteria. All of the simulations

are performed in Matlab 2019b on a CPU architecture of i7-4820K (3.7 GHz).

Note we divide feasibility of the solution into two parts, one is feasibility with respect to the constraint function g and the other is with respect to the dynamics f . SQP handles them as inequalities (for g) and equalities (for f) constraints, whereas DDP-based methods can implicitly satisfy dynamics since they are used during the optimization process.

1) *Exit criteria*: The exit condition of optimization was based on two criteria as shown in Table I. One was constraint satisfaction, where 1×10^{-7} was used for all the algorithms. The other was an optimality criterion. For the DDP based

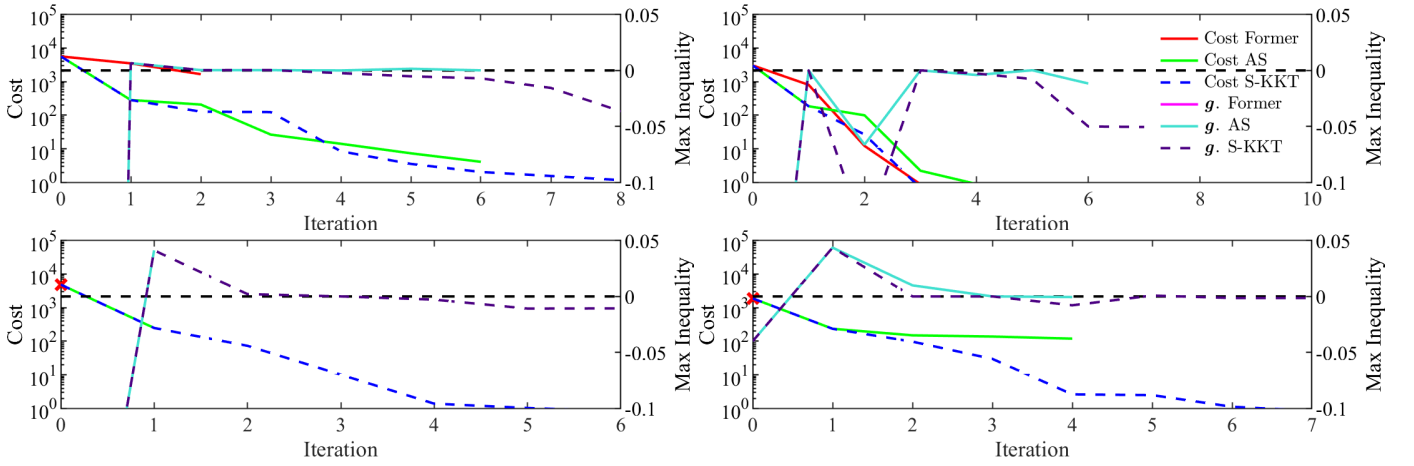


Fig. 6: Cost and max. inequality constraints of quadroter task.

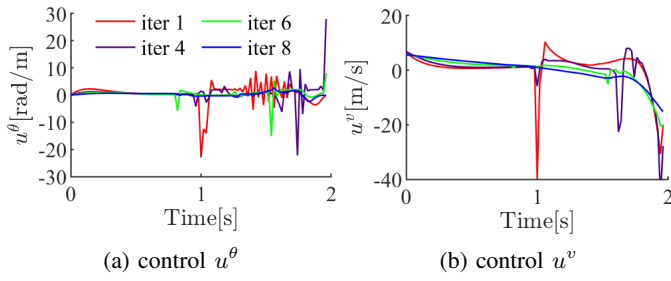


Fig. 7: control over iteration

TABLE I: Exit criteria

(a) Exit criteria for single algorithms.

criterion	SQP	S-KKT	AL-DDP
cnst. satisfaction	1E-07	1E-07	1E-07
closeness to optimal solution	opt. tolerance 1E-2	change in cost 8E-2	change in cost 8E-2

(b) Exit criteria for combination algorithms.

stage	AL-SKKT	AL-DDP
first	cnst. satisfaction: 1E-2	
AL-DDP	change in cost: 1	
final	cnst. satisfaction: 1E-7	
optimization	opt. tolerance: 1E-2	change in cost: 8E-2

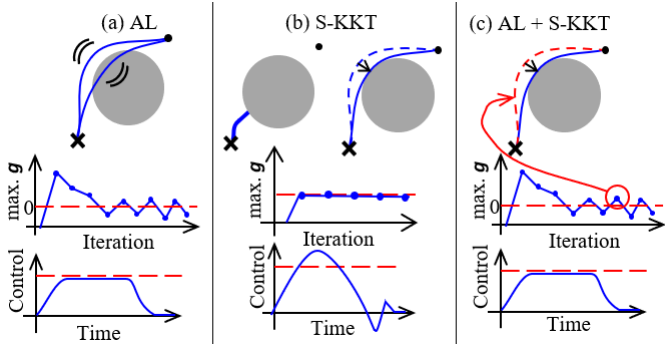


Fig. 8: Concept of combining AL and S-KKT. (a) AL-DDP shows oscillatory behavior around the boundary and take many iterations to keep feasibility. (b) S-KKT get stuck or infeasible when large control is required. This situation happens when goal state is far from initial trajectory or large control is required to dodge the obstacle. Be able to keep feasibility. (c) S-KKT is good at pushing a trajectory which is close to the optimal. Obtain initial trajectory from AL and optimize the trajectory more to the optimal by S-KKT.

methods, we used the change in the optimization objective between iterations, set to 8×10^{-2} . For SQP, we used an optimality condition shown in the first equation of (10). This condition was set by choosing the Matlab `fmincon` option `OptimalityTolerance` to be 1×10^{-2} . We first set the

value to be 8×10^{-2} which is the same as that of other DDP based methods. However, SQP stopped its optimization process reaching local minima in the early iterations for several examples, which kept the cost of SQP relatively much higher. In the 2D car and the quadroter case for example, the cost was about a hundred times higher than S-KKT. Therefore, we made the criteria smaller to further the SQP optimization process. When using the change of objective function instead of the optimality tolerance in SQP, we observed that the condition was also satisfied in the early iterations of the optimization, but with a large constraint violation. This means that only the constraint satisfaction was working effectively as the exit condition. Thus, we decided to use the optimality tolerance for SQP. For AL-SQP and AL-S-KKT, we also have conditions on exiting the AL optimization scheme and switching to the next scheme as shown in Table Ib). In lieu of fairness, we decided to keep this "switching condition" and other AL parameters the same between both algorithms even if they may have benefited with different conditions for the overall convergence requirements. For these AL schemes, the constraint satisfaction tolerance was 1×10^{-2} and the bound on the change of the cost was 1.

2) *Cart Pole*: Table II shows the results of the simulations for balancing a cart pole system. The system has four dimen-

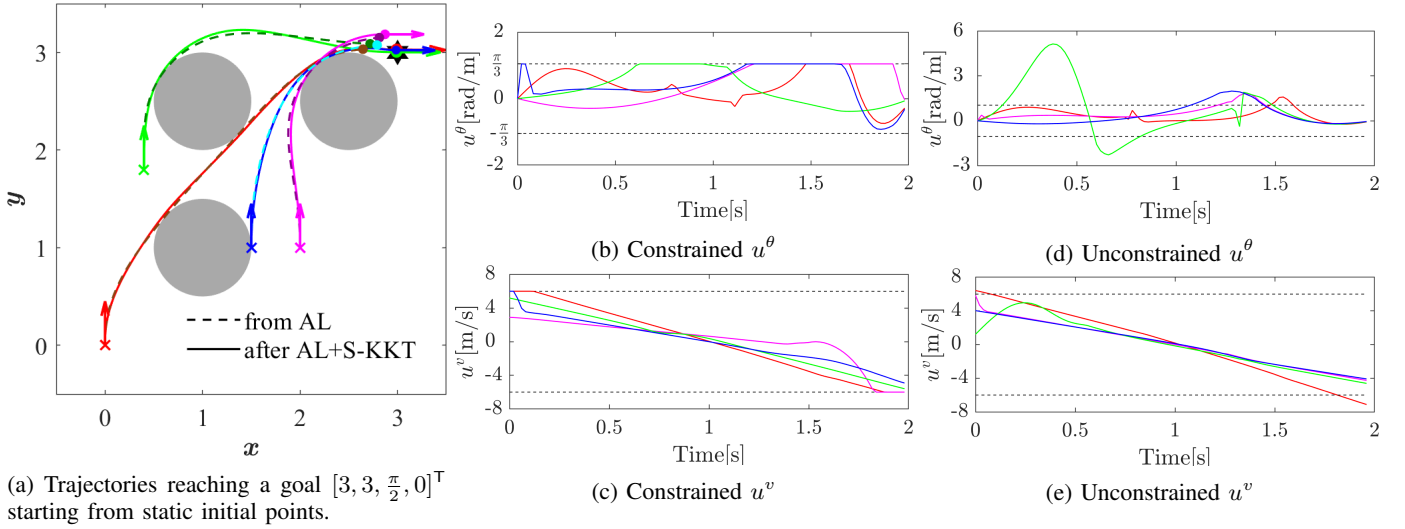


Fig. 9: Results from combined algorithm. In Fig. 9a, position and orientation at initial and final time steps from final result are shown by points and arrows. For AL, only final positions are plotted as circles, and arrows are omitted to make the figure easy to see.

TABLE II: Performance metrics for a cart pole system until convergence.

H	Metric	SQP	S-KKT	AL	AL-SQP	AL-S-KKT
100	Cost	3.11	5.90	5.97	3.06	6.06
	Time	12.3	7.38	5.32	11.7	4.70
	Feas. (g)	0	0	1.89E-04	0	0
	Feas. (f)	1.90E-03	0	0	3.19E-04	0
200	Cost	2.80	7.77	5.81	2.77	5.28
	Time	52.2	12.0	10.7	48.5	12.1
	Feas. (g)	0	0	2.50E-04	0	0
	Feas. (f)	2.78E-05	0	0	1.98E-04	0

TABLE III: Performance metrics for a cart pole system with time budget.

H	Metric	SQP	S-KKT	AL	AL-SQP	AL-S-KKT
100	Cost	3.53	5.90	5.97	3.18	6.06
	Time	6	6	5.25	6	4.69
	Feas. (g)	0	0	1.89E-04	0	0
	Feas. (f)	4.12E-03	0	0	4.83E-03	0
200	Cost	7.21	8.37	7.33	5.80	7.14
	Time	6	6	6	6	6
	Feas. (g)	0	0	3.34E-04	5.50E-06	0
	Feas. (f)	1.22E-03	3.55E-06	0	3.51E-02	0

sion of state \mathbf{x} , that is position of the cart x , its velocity \dot{x} , angle of the pendulum θ , and angular velocity $\dot{\theta}$. The control of the system is thrust force u applied to the cart. The dynamics is given as follows:

$$\begin{aligned}\ddot{x}_k &= \frac{u_k - b\dot{x}_k + m(l + \dot{\theta}_k^2 - g \cos \theta_k) \sin \theta_k}{(M + m \sin^2 \theta_k)}, \\ \ddot{\theta}_k &= \frac{g(M + m) \sin \theta_k - (u - b\dot{x}_k + ml\dot{\theta}_k^2 \sin \theta_k) \cos \theta_k}{l(M + m \sin^2 \theta_k)},\end{aligned}\quad (72)$$

where M is a mass of the cart, m is that of pendulum, l is a length of the arm of the pendulum, g is gravitational acceleration, and b is a coefficient of friction between the car and the floor. The problem has constraints in the position and angle:

$$\mathbf{g}_{\text{cp}} = \begin{bmatrix} x^2 - x_{\text{lim}}^2 \\ \theta - \theta_{\text{lim}} \end{bmatrix} \leq \mathbf{0} \quad (73)$$

Pure SQP performed the slowest with dynamics violation, although it achieved a very low cost. It required a much longer time for a longer time horizon compared to other methods. This is understandable because in SQP, a longer time horizon corresponds to a larger matrix (which needs to be

inverted) containing the equality constraints for the dynamics. S-KKT also takes time and it accrues a high cost compared to SQP. However, it does satisfy feasibility. AL-DDP on its own cannot reach the same levels of constraint satisfaction as S-KKT, which makes sense since the AL approach oscillates near the constraint bounds, but converges faster. When pairing AL with SQP, there is no significant change compared to original SQP. Pairing AL with S-KKT, however, we see an improvement. In the case of $H = 100$, compared to S-KKT, AL-S-KKT converges faster to an almost equally low cost. In the case of $H = 200$, AL-S-KKT takes slightly longer time, but converges to a lower cost. Compared to AL, AL-S-KKT takes a long time, but satisfies feasibility. From Table III, we can see the longer time horizon decreases the performance of SQP in terms of speed and constraint satisfaction, where AL-S-KKT is not affected as much. In S-KKT, there is a small violation of constraint possibly from the linearization error of the constraint function. The solution may satisfy the linearized constraint in (14), but not the original one. The error decreases as δu decreases, but if we use a time budget and stop the optimization process before convergence, there is a possibility that the solution has a small violation.

3) *2D car*: We use the same problem setting as V-A1. For these metrics we initialize the problem with six different starting points and take the average of the cost, time, and feasibility. The time step used was $dt = 0.02$ s. Table IV shows the result when we let run the algorithm until convergence, and Table V shows the result under time budget. In the case of $H = 100$, time budget was 3 s, and when $H = 200$, it was 6 s. In this example algorithms behave similarly as the example of a cart pole, and combination methods show their performance more clearly in terms of speed.

TABLE IV: Performance metrics for a 2D car system until convergence.

H	Metric	SQP	S-KKT	AL	AL-SQP	AL-S-KKT
100	Cost	2.85	2.58	2.55	2.39	2.45
	Time	11.1	5.51	5.69	5.77	2.41
	Feas. g	0	0	4.05E-04	0	0
	Feas. f	1.30E-06	0	0	5.01E-08	0
200	Cost	1.66	1.20	1.12	0.995	1.05
	Time	67.3	11.6	10.6	38.0	3.98
	Feas. g	0	0	1.26E-04	-7.63E-08	0
	Feas. f	2.26E-05	0	0	4.63E-08	0

TABLE V: Performance metrics for a 2D car system with time budget.

H	Metric	SQP	S-KKT	AL	AL-SQP	AL-S-KKT
100	Cost	25.3	22.5	3.13	2.49	2.44
	Time	3	2.77	3	3	2.36
	Feas. g	0	0	0	0	0
	Feas. f	1.02E-03	0	0	2.53E-05	0
200	Cost	135	43.2	1.71	1.80	1.92
	Time	6	6	6	6	3.88
	Feas. g	0	0	1.73E-03	0	0
	Feas. f	1.22E-02	0	0	1.10E-05	0

4) *Quadroter*: In this example, we used same problem setting as Section V-A2 initialized with four different static hovering points, and take the average of performance metrics as we did in the 2D car example. We set a time step of $dt = 0.01$. As we can see from the results shown in Table VI, SQP suffers from increase of dimension of the problem resulting in a much longer computational time. AL in the case of $H = 300$, could not get out from its inner optimization loop, and could not converge. We filled the corresponding table with “N/A”. Our S-KKT and AL-S-KKT, however could keep its stability and feasibility. In addition, they achieved a low cost in a short time. Table VII shows the result from the same problem under a time budget. For $H = 200$, the time budget was 6 s and for $H = 300$ it was 10 s. Single SQP took such a long time that it could not perform one single iteration, resulting in very high cost. We have observed that our AL-S-KKT lost its speed performance affected by the first AL optimization process. AL consumed most of the time budget, allowing S-KKT only one or two iterations. We believe that more investigation or tuning of AL will make our AL-S-KKT much better.

TABLE VI: Performance metrics for a quadroter system until convergence.

H	Metric	SQP	S-KKT	AL	AL-SQP	AL-S-KKT
200	Cost	5.87	7.95	8.10	5.5	7.03
	Time	748	12.3	23.8	790	10.7
	Feas. g	0	0	0	0	0
	Feas. f	1.16E-05	0	0	2.84E-05	0
300	Cost	5.91	5.99	N/A	5.37	6.88
	Time	2.55E03	21.9	N/A	2.42E03	14.9
	Feas. g	0	0	N/A	0	0
	Feas. f	1.28E-05	0	N/A	2.08E-05	0

TABLE VII: Performance metrics for a quadroter system with time budget.

H	Metric	SQP	S-KKT	AL	AL-SQP	AL-S-KKT
200	Cost	2.43E03	26.1	10.7	8.12	7.48
	Time	6	5.68	6	6	5.91
	Feas. g	0	0	0	0	0
	Feas. f	1.86E-03	0	0	7.99E-04	0
300	Cost	2.86E03	7.52	7.91	8.01	7.78
	Time	10	10	10	10	10
	Feas. g	0	0	0	0	0
	Feas. f	2.50E-03	0	0	6.85E-09	0

VI. CONCLUSION

In this paper we have introduced novel constrained trajectory optimization methods that outperform previous versions of constrained DDP. Some key ideas in this paper rely on the combination of slack variables together with augmented Lagrangian method and the KKT conditions. In particular,

- Slack variables are an effective way to get lower cost with respect to alternative algorithms relying on the active set method.
- The S-KKT method is able to handle both state and control constraints in cases where the feasibility set is small.
- The S-KKT methods is more robust to initial conditions of the state trajectory.
- AL is very fast for first few iterations but get slow when it comes close to constraints and sometimes violate constraints. Whereas S-KKT takes time in one iteration, but can keep feasibility in a few iterations. By combining them we may be able to compensate for weakness of both and have a better algorithm.

Future directions will include mechanisms for uncertainty representations and learning, and development of chance constrained trajectory optimization algorithms that have the benefits of the fast convergence of the proposed algorithms.

APPENDIX A ON THE AUGMENTED LAGRANGIAN

The penalty functions in (11) must be such that $\mathcal{P}'(y, \lambda, \mu) := \frac{\partial}{\partial y} \mathcal{P}(y, \lambda, \mu)$ is continuous for all $y \in \mathbb{R}$, $\lambda, \mu \in \mathbb{R}_{++}$ and: (i) $\mathcal{P}'(y, \lambda, \mu) \geq 0$, (ii) $\lim_{k \rightarrow \infty} \mu_{(k)} = \infty$ and $\lim_{k \rightarrow \infty} \lambda_{(k)} = \lambda > 0$ imply that $\lim_{k \rightarrow \infty} \mathcal{P}'(y_{(k)}, \lambda_{(k)}, \mu_{(k)}) = \infty$, (iii)

$\lim_{k \rightarrow \infty} \mu_{(k)} = \infty$ and $\lim_{k \rightarrow \infty} \lambda_{(k)} = \lambda < 0$ imply that $\lim_{k \rightarrow \infty} \mathcal{P}^l(y_{(k)}, \lambda_{(k)}, \mu_{(k)}) = 0$.

REFERENCES

- [1] Dimitri P Bertsekas. *Dynamic programming and optimal control*, volume 1. Athena scientific Belmont, MA, 1995.
- [2] Ernesto G Birgin, Romulo A Castillo, and José Mario Martínez. Numerical comparison of augmented lagrangian algorithms for nonconvex problems. *Computational Optimization and Applications*, 31(1):31–55, 2005.
- [3] Markus Gifftthaler and Jonas Buchli. A projection approach to equality constrained iterative linear quadratic optimal control. In *2017 IEEE-RAS 17th International Conference on Humanoid Robotics (Humanoids)*, pages 61–66. IEEE, 2017.
- [4] Taylor A Howell, Brian E Jackson, and Zachary Manchester. Altro: A fast solver for constrained trajectory optimization. In *2019 IEEE International Conference on Intelligent Robots and Systems, IEEE*, 2019.
- [5] David H. Jacobson and David Q. Mayne. *Differential dynamic programming*. Elsevier, 1970. ISBN 0-444-00070-4.
- [6] Marin B Kobilarov and Jerrold E Marsden. Discrete geometric optimal control on lie groups. *IEEE Transactions on Robotics*, 27(4):641–655, 2011.
- [7] Vikash Kumar, Emanuel Todorov, and Sergey Levine. Optimal control with learned local models: Application to dexterous manipulation. In *2016 IEEE International Conference on Robotics and Automation (ICRA)*, pages 378–383. IEEE, 2016.
- [8] Gregory Lantoine and Ryan Russell. A hybrid differential dynamic programming algorithm for robust low-thrust optimization. In *AIAA/AAS Astrodynamics Specialist Conference and Exhibit*, page 6615, 2008.
- [9] Sergey Levine and Pieter Abbeel. Learning neural network policies with guided policy search under unknown dynamics. In *Advances in Neural Information Processing Systems*, pages 1071–1079, 2014.
- [10] Weiwei Li and Emanuel Todorov. Iterative linear quadratic regulator design for nonlinear biological movement systems. In *ICINCO (1)*, pages 222–229, 2004.
- [11] L-Z Liao and Christine A Shoemaker. Convergence in unconstrained discrete-time differential dynamic programming. *IEEE Transactions on Automatic Control*, 36(6):692–706, 1991.
- [12] T.C. Lin and J.S. Arora. Differential dynamic programming technique for constrained optimal control. *Computational Mechanics*, 9:27–40, 1991.
- [13] Teppo Luukkonen. Modelling and control of quadcopter. *Independent research project in applied mathematics, Espoo*, 2011.
- [14] Katja Mombaur. Using optimization to create self-stable human-like running. *Robotica*, 27(3):321–330, 2009.
- [15] Jun Morimoto, Garth Zeglin, and Christopher G Atkeson. Minimax differential dynamic programming: Application to a biped walking robot. In *Proceedings 2003 IEEE/RSJ International Conference on Intelligent Robots and Systems (IROS 2003)(Cat. No. 03CH37453)*, volume 2, pages 1927–1932. IEEE, 2003.
- [16] Daniel M Murray and Sidney J Yakowitz. Constrained differential dynamic programming and its application to multireservoir control. *Water Resources Research*, 15(5):1017–1027, 1979.
- [17] Jorge Nocedal and Stephen Wright. *Numerical optimization*. Springer Science & Business Media, 2006.
- [18] Brian Plancher, Zachary Manchester, and Scott Kuindersma. Constrained unscented dynamic programming. In *2017 IEEE/RSJ International Conference on Intelligent Robots and Systems (IROS)*, pages 5674–5680. IEEE, 2017.
- [19] Yuval Tassa, Tom Erez, and Emanuel Todorov. Synthesis and stabilization of complex behaviors through online trajectory optimization. In *2012 IEEE/RSJ International Conference on Intelligent Robots and Systems*, pages 4906–4913. IEEE, 2012.
- [20] Yuval Tassa, Nicolas Mansard, and Emo Todorov. Control-limited differential dynamic programming. In *2014 IEEE International Conference on Robotics and Automation (ICRA)*, pages 1168–1175. IEEE, 2014.
- [21] Zhaoming Xie, C Karen Liu, and Kris Hauser. Differential dynamic programming with nonlinear constraints. In *2017 IEEE International Conference on Robotics and Automation (ICRA)*, pages 695–702. IEEE, 2017.